Journal of Biomolecular NMR, **15:** 157–168, 1999.
KLUWER/ESCOM

Novel multi-dimensional heteronuclear NMR techniques for the study of ^{13}C-*O*-acetylated oligosaccharides: Expanding the dimensions for carbohydrate structures

David N.M. Jones[a,*] & Brad Bendiak[b]
Departments of [a]Pharmacology and [b]Cellular and Structural Biology, University of Colorado Health Sciences Center, Box C236, 4200 East Ninth Avenue, Denver, CO 80262, U.S.A.

Received 17 June 1999; Accepted 30 August 1999

Key words: C-13 labeling, carbohydrates, coupling constants, heteronuclear Hartmann–Hahn, *O*-acetylation, oligosaccharides

Abstract

Complex carbohydrates have critical roles in a wide variety of biological processes. An understanding of the molecular mechanisms that underlie these processes is essential in the development of novel oligosaccharide-based therapeutic strategies. Unfortunately, obtaining detailed structural information for larger oligosaccharides (>10 residues) can be exceedingly difficult, especially where the amount of sample available is limited. Here we demonstrate the application of ^{13}C *O*-acetylation in combination with novel NMR experiments to obtain much of the information required to characterize the primary structure of oligosaccharides. (H)C_{Me}COH-HEHAHA and H(C_{Me})COH-HEHAHA experiments are presented that use heteronuclear Hartmann–Hahn transfer to correlate the acetyl groups with sugar ring protons in peracetylated oligosaccharides. The in-phase, pure absorption nature of the correlation peaks in these experiments allows measurement of both chemical shifts and, importantly, ^{1}H-^{1}H coupling constants that are used to define the stereochemistry of the sugar ring. The (HC_{Me})COH and (HC_{Me})COH-RELAY experiments provide additional methods for obtaining chemical shift assignments for larger oligosaccharides to define the sites of glycosidic linkages from the patterns of acetylation.

Introduction

Complex carbohydrates are important components of nearly all biological systems and play essential roles in a variety of processes including mammalian embryonic development (Metzler et al., 1994), intercellular recognition events (Homeister et al., 1998), regulation and mediation of the immune response (Hennet et al., 1998), plant cell signaling (Darvill et al., 1994) and cytokine localization (Hileman et al., 1998). Changes in the native structures of mammalian glycoproteins and glycolipid oligosaccharides have been shown to correlate with various cancer cell metastases (Hounsell et al., 1997) and inherited diseases (Tan et al., 1996; Chui et al., 1997). Consequently, oligosaccharides are becoming increasingly important targets in the development of novel therapeutic strategies.

The primary structure of an oligosaccharide can be defined by determining the identity of each monomer, the stereochemistry at the anomeric position and the location of the glycosidic linkages between the monomers. Unlike proteins and nucleic acids, the building blocks that make up oligosaccharides may differ from each other solely in the nature of their stereochemistry, and the patterns of inter-monomer linkages can be extremely heterogeneous. Consequently, determining the structures of complex oligosaccharides is a difficult problem.

NMR spectroscopy can be used to obtain much of the information needed to characterize the structures of oligosaccharides. In particular, the values of the ^{1}H-^{1}H *J*-coupling constants can be used to deter-

*To whom correspondence should be addressed. E-mail: David.Jones@UCHSC.edu.

mine the relative axial/equatorial relationships of the sugar ring protons which are unique for each type of monosaccharide. However, NMR studies of oligosaccharides are complicated by the following factors: first, the sugar ring protons, other than the anomeric protons, resonate over a very narrow spectral region (approximately 3.3–4.3 ppm) which may make it difficult to obtain chemical shift assignments and accurate measurements of ^{1}H-^{1}H coupling constants because of the severe resonance overlap; second, it is often not possible to unambiguously establish the ring positions of linkages between the monosaccharides, as the strongest NOEs may not be between protons directly across the glycosidic linkage. In addition, the measurement of $^{3}J_{CH}$ across the glycosidic bond to establish sequential linkages is a relatively insensitive technique for natural abundance oligosaccharides and often requires biosynthetic enrichment with ^{13}C; third, the limited chemical-shift dispersion in the spectrum of oligosaccharides leads to strong coupling effects between some ring protons which may make it difficult to determine accurate values of J_{HH}.

Biosynthetic enrichment with ^{13}C can be used to reduce the problems of resonance overlap. However, this option is often not available for many interesting and important oligosaccharides such as those isolated from human cells in diseases such as cancer. In these cases the limited amounts of material available effectively restrict the investigator to the use of ^{1}H-^{1}H experiments.

^{13}C *O*-acetylation is a powerful tool for reducing the problem of spectral overlap for oligosaccharides. This approach has particular advantages compared to biosynthetic ^{13}C labeling of the sugar backbone: (i) it introduces two ^{13}C nuclei that have very different chemical shifts which can be manipulated independently; (ii) *O*-acetylation induces changes in the chemical shifts of the ring protons, which significantly improves the spectral resolution in the ^{1}H dimension. This is in contrast to biosynthetic labeling which produces no change; (iii) most importantly, ^{13}C *O*-acetylation can be used for any oligosaccharide, regardless of its source, and is not limited to samples produced from bacterial or cell cultures.

Initial studies of peracetylated oligosaccharides that were ^{13}C-labeled only at the carbonyl position used heteronuclear COSY and HMBC experiments to correlate ^{13}CO-^{1}H^{ring} pairs (Bendiak, 1999). These experiments established the range of values for the $^{3}J_{CO-H}$ coupling as 2.5–4.7 Hz and confirmed that longer range couplings to ring protons other than at the site of acetylation were very small and not observable. From these experiments it was possible to identify those protons at positions which are not acetylated: namely the anomeric proton, the proton at the position of cyclization (H5 for pyranose) and the proton at the position of the *glycosidic linkage*. This approach works well for smaller oligosaccharides (<8–10 sugars) but for larger molecules the increased resonance overlap limits the information that can be obtained.

We present here a set of heteronuclear multidimensional NMR experiments for the study of larger oligosaccharides prepared with doubly ^{13}C-labeled acetyl groups. These experiments establish correlations between protons on the sugar rings and the acetyl groups in three independent dimensions, namely the ^{13}C methyl ($^{13}C^{Me}$) and ^{13}C-carbonyl carbons (^{13}CO), and the methyl protons ($^{1}H^{Me}$). The (H)C_{Me}COH-HEHAHA and H(C_{Me})COH-HEHAHA experiments generate in-phase, pure-absorption spectra that can be used to obtain almost all the chemical shift assignments and ^{1}H-^{1}H *J*-coupling constants for individual sugar rings. The (HC_{Me})COH correlates the acetyl group with the proton at the site of acetylation and the (HC_{Me})COH-RELAY establishes correlations to protons immediately adjacent to the site of acetylation. Together these latter two experiments provide additional methods for obtaining unambiguous chemical shift assignments. We demonstrate the application of these techniques to a tetrasaccharide (1):

$$\underset{A}{\alpha\text{-Glucose}}\ (1\text{-}3)\ \underset{B}{\alpha\text{-Glucose}}\ (1\text{-}4)\ \underset{C}{\alpha\text{-Glucose}}\ (1\text{-}3)\ \underset{D}{\text{Glucitol}} \quad (1)$$

The high resolution and chemical shift dispersion in these experiments suggest that it may be possible to obtain structural information for oligosaccharides containing up to 15–20 sugars.

Materials and methods

Samples of peracetylated oligosaccharide (1) for NMR spectroscopy were prepared as previously described (Bendiak, 1999) except that acetic anhydride (1,1′,2,2′-$^{13}C_4$, Cambridge Isotopes) was used instead. Samples were dissolved in 99.996% $CDCl_3$ (Aldrich) to a final concentration of 0.2 mM.

All NMR experiments were performed on a Varian Inova spectrometer equipped with Z-axis gradients and operating at a ^{1}H frequency of 500 MHz. All experiments were recorded at 27 °C using a 5 mm triple resonance probe. The spectrometer was configured with pulse shaping capability on both the

^{1}H and ^{13}C transmitter channels and in addition had pulse shaping capability on the gradient channel. All the shaped pulse waveforms were generated using the Varian software 'Pbox' and verified in the program 'Pulsetool' and checked experimentally. Gradient waveforms were generated from in-house programs. Data were processed using Felix (MSI Inc.). In all experiments a mild composite sinebell/Gaussian window function (Ernst et al., 1987) was applied in all dimensions prior to Fourier transformation.

Results

(H)C$_{Me}$COH-HEHAHA and H(C$_{Me}$)COH-HEHAHA

The (H)C$_{Me}$COH-HEHAHA and H(C$_{Me}$)COH-HEHAHA were designed to correlate the acetyl groups of peracetylated oligosaccharides with the protons on the sugar ring. In previous studies we used heteronuclear COSY experiments to establish these correlations (Bendiak, 1999). However, these COSY-based experiments retain the antiphase splitting in the correlation peaks and are less useful for studying larger, more complex systems, especially when the digital resolution is limited in the indirectly detected dimensions in 3D experiments. The (H)C$_{Me}$COH-HEHAHA and H(C$_{Me}$)COH-HEHAHA use heteronuclear Hartmann–Hahn mixing (Braunschweiler and Ernst, 1983) to generate in-phase, pure-absorption correlations between doubly ^{13}C-labeled acetyl groups and the protons of the sugar ring. This avoids the cancellation problems that arise in COSY-type experiments and results in spectra with high resolution and relatively high sensitivity. The principles of these experiments are similar to sequences developed for the study of proteins (Majumdar et al., 1993; Richardson et al., 1993; Wang and Zuiderweg, 1995; Zuiderweg et al., 1996) and nucleic acids (Kellogg, 1992; Kellogg and Schweitzer, 1993; Nikonowicz and Pardi, 1993; Schweitzer et al., 1995; Wijmenga et al., 1995; Sklenar et al., 1996) and so only a brief description of the experiments is presented here.

(H)C$_{Me}$COH-HEHAHA

The (H)C$_{Me}$COH-HEHAHA (Figure 1A) correlates the ^{13}C^{Me} and ^{13}CO of the acetyl groups with the protons on the sugar ring. The experiment starts with a selective 90° e-burp-2 pulse (Geen and Freeman, 1991) on the ^{1}H^{Me} of the acetyl groups. In the following INEPT transfer period (2∗Δ1) the 180° pulse on the ^{13}C^{Me} is applied as a selective re-burp pulse (Geen and Freeman, 1991) to minimize sensitivity losses that may result from direct transfer of ^{1}H^{Me} magnetization to ^{13}CO through the $^{3}J_{CO-HMe}$ coupling (∼7 Hz). Artifacts due to imperfections in the 180° pulses are removed by the gradients g1. Immediately after the 90° ^{1}H pulse at the end of this INEPT period the transmitter frequency is switched to the middle of the ^{1}H spectrum. At this point the coherence from ^{1}H nuclei that is not attached to the ^{13}C^{Me} is dephased by the gradient g2. Following a selective 90° pulse on the ^{13}C^{Me} (e-burp-2), magnetization evolves during the evolution period t_1. In pulse sequences designed for proteins it would be usual to combine this evolution period with the following transfer step. However, the small spectral width in the ^{13}C^{Me} dimension (2–3 ppm) results in a large time increment in t_1 which severely limits the number of increments that can be recorded using such a combined approach. The effects of couplings to ^{1}H and ^{13}CO are removed by application of 180° pulses in the middle of the evolution time. The pulse on the ^{13}CO frequencies is applied with a seduce-1 profile (McCoy and Mueller, 1993), phase modulated to produce inversion at the ^{13}CO position (Boyd and Soffe, 1989; Patt, 1992). The Bloch–Siegert phase shifts induced by this pulse are compensated for by making corrections to the phase of the ^{13}C^{Me} 90° pulse at the beginning of the evolution period. During the following INEPT period (2∗Δ3) magnetization is transferred from the ^{13}C^{Me} to ^{13}CO while simultaneously allowing the ^{1}H-^{13}C^{Me} coupling to refocus for a period of $1/2J_{CMe-H}$ before turning on the proton decoupler. Inversion of ^{13}C^{Me} and ^{13}CO is achieved with a single hyperbolic secant 180° pulse (Silver et al., 1984; Baum et al., 1985), phase modulated so it is centered in the middle of the ^{13}C spectrum (in Figure 1A this pulse marked (c) is depicted as separate pulses on ^{13}C^{Me} and ^{13}CO but is applied as a single pulse). This pulse introduces a frequency-dependent quadratic phase shift on the transverse magnetization which is compensated for by applying the same pulse at the end of the second period Δ3 at position (d) (Hwang and Shaka, 1995; Kupce and Freeman, 1997). After a selective 90° pulse (Q5 Gaussian (Emsley and Bodenhausen, 1992)) on ^{13}C^{Me}, the frequency of the ^{13}C transmitter is switched to the center of the ^{13}CO region. The following period 2∗Δ3 is used to refocus the magnetization into pure absorption CO_x after which it evolves during t_2. Again the refocusing and detection periods

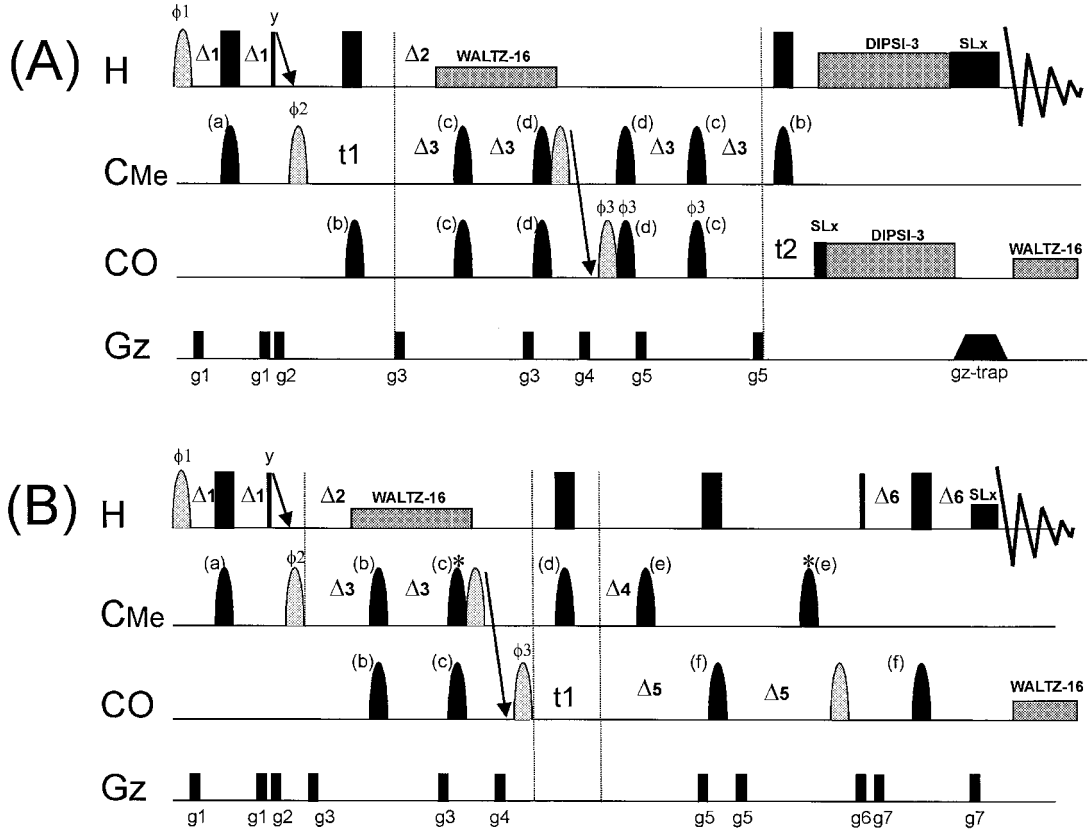

Figure 1. Pulse sequences used to record (A) the (H)C_{Me}COH-HEHAHA, and (B) the (HC_{Me})COH. In both schemes wide solid bars represent hard 180° pulses and narrow bars represent hard 90° pulses. Shaped 180° pulses are represented as solid filled curves and shaped 90° pulses are represented as gray shaded curves. In all experiments the ^{1}H transmitter is initially placed at the center of the methyl protons (2.2 ppm) and the ^{13}C transmitter is placed at the center of the methyl carbons (21.3 ppm). Subsequently the ^{1}H transmitter is moved to the center of the ^{1}H spectrum (3.9 ppm) and the ^{13}C transmitter is moved to the center of the ^{13}CO region (170 ppm) at the points indicated by the arrows. The selective pulse on the $^{1}H^{Me}$ at the beginning of each experiment has a duration of 5.75 ms and has an e-burp-2 profile (Geen and Freeman, 1991). Selective ^{13}C 90° pulses that act on Z magnetization are applied for 600 μs with an e-burp-2 profile. Selective ^{13}C 90° pulses that act on transverse magnetization are applied as a 600 μs Q5 Gaussian pulse (Emsley and Bodenhausen, 1992). Decoupling of ^{1}H during the period (2∗Δ3) and of ^{13}CO during acquisition is achieved with a WALTZ-16 decoupling scheme (Shaka et al., 1983) applied with field strengths of 4.1 kHz and 2.2 kHz, respectively. In those cases where a hyperbolic secant pulse is applied to transverse magnetization the delays on either side of each pulse, including those for power switching and other programming events, are carefully arranged to be exactly symmetrical to avoid any subsequent phase errors. Other details for each experiment are discussed separately. (A) In the (H)C_{Me}COH-HEHAHA the pulse shapes and lengths are: (a) reburp-2 (Geen and Freeman, 1991), 600 μs; (b) seduce-1 (McCoy and Mueller, 1993), 250 μs, phase modulated by 148.9 ppm (Boyd and Soffe, 1989; Patt, 1992); (c) hyperbolic secant (Silver et al., 1984; Baum et al., 1985), 450 μs, phase modulated by 70 ppm; (d) is the same as pulse (c) and is applied to refocus the quadratic shift. In the figure pulses (c) and (d) are represented as separate pulses on the $^{13}C^{Me}$ and ^{13}CO resonances but in practice are applied as a single pulse. Heteronuclear Hartmann–Hahn mixing uses a DIPSI-3 sequence (Shaka et al., 1988; Brown and Sanctuary, 1991; Majumdar et al., 1993) with a field strength of 3.05 kHz applied for a period of 141 ms. Other delays were $\Delta1 = 1.9$ ms, $\Delta2 = 3.8$ ms, $\Delta3 = 4.5$ ms. The spin-lock pulse (SLx) at the end of the mixing period was applied for a period of 30 ms at the same time as the trapezoidally shaped gradient pulse (Davis et al., 1993). This gradient, gz-trap, had a maximum strength of 4 G/cm and the period used to ramp the gradient up to its maximum strength (and subsequently back down to zero) was 25% of the total gradient duration (30 ms). The durations and strengths of the other gradients were g1 = (0.4 ms, 16 G/cm), g2 = (0.4 ms, 20 G/cm), g3 = (0.4 ms, 18 G/cm), g4 = (0.4 ms, 16 G/cm), g5 = (0.5 ms, 18 G/cm). The phase cycling used was $\phi1 = 4(x),4(-x)$, $\phi2$ = (x, x, −x,−x), $\phi3$ = (x, −x), rec = (x, −x, −x, x, −x, x, x, −x). Quadrature detection in the indirect dimensions used States-TPPI (Marion et al., 1989) of $\phi2$ for F1 and of $\phi3$ for F2. (B) In the (HC_{Me})COH and (HC_{Me})COH-RELAY the shapes and durations of pulses are (a) reburp, 600 μs; (b) and (c) hyperbolic secant, 450 μs, phase modulated by 70 ppm; (d) seduce-1, 250 μs, phase modulated by 148.9 ppm; (e) reburp, 600 μs, phase modulated by 148.9 ppm; (f) reburp, 600 μs. Bloch–Siegert compensating pulses are indicated with a ∗. The delays were $\Delta1 = 1.9$ ms, $\Delta2 = 3.8$ ms, $\Delta3 = 4.5$ ms, $\Delta4 = 4.5$ ms, $\Delta5 = 65$ ms, $\Delta6 = 65$ ms. The gradient strengths and durations are g1 = (0.4 ms, 16 G/cm), g2 = (0.4 ms, 20 G/cm), g3 = (0.4 ms, 18 G/cm), g4 = (0.4 ms, 16 G/cm), g5 = (0.5 ms, 18 G/cm), g6 = (0.4 ms, 10 G/cm), g7 = (0.5 ms, 20 G/cm). The phase cycle is $\phi1 = 4(x),4(-x)$, $\phi2$ = (x, x, −x,−x), $\phi3$ = (x, −x), rec = (x, −x, −x, x, −x, x, x, −x) and quadrature detection in F1 is obtained by States-TPPI of $\phi3$. In the (HC_{Me})COH-RELAY sequence the final ^{1}H spin-lock pulse (SLx) is replaced with a hard 90° pulse with phase = x as described in the text.

are separate because of the small spectral width in the ^{13}CO dimension (2–3 ppm).

In-phase CO_x magnetization is transferred to the ring protons, where it is detected, by Hartmann–Hahn cross-polarization (Braunschweiler and Ernst, 1983), using a DIPSI-3 mixing sequence (Shaka et al., 1988; Brown and Sanctuary, 1991; Majumdar et al., 1993). Optimal transfer from the acetyl group to the ring protons requires a mixing period of ∼130–140 ms. However, during this relatively long mixing period significant magnetization transfer occurs to other protons in the sugar ring through the more efficient homonuclear Hartman–Hahn transfer process (Bearden and Brown, 1989; Zuiderweg, 1990; Brown and Sanctuary, 1991; Ernst et al., 1991). The ^{1}H-^{1}H couplings (∼3–12 Hz) are generally larger than the ^{13}CO-^{1}H couplings (2.5–4.7 Hz) and homonuclear transfer is proportional to J_{HH} whereas heteronuclear transfer is proportional to $J_{CH}/2$ (Zuiderweg, 1990). Therefore any magnetization that is transferred from ^{13}CO to $^{1}H^{ring}$ is efficiently transferred to other ring protons. In the (HC_{Me})COH-TOCSY spectrum of this oligosaccharide, recorded with similar spin-locking field strengths, we observe significant transfer to almost all the other ring protons using mixing times of ∼15 ms (data not shown).

Figure 2A shows the ^{13}CO-$^{1}H^{ring}$ spectrum recorded using a 2D version of the (H)C_{Me}COH-HEHAHA sequence of Figure 1A. Each acetyl ^{13}CO group shows correlations to a number of protons within the sugar ring as a result of homonuclear Hartmann–Hahn transfer. These additional correlations provide almost complete sub-spectra of individual sugar ring spin systems originating from each acetyl substituent. The resulting correlations are in-phase and pure absorption in all dimensions. As a result, almost all the correlations are well resolved for this small oligosaccharide. Any ambiguities that do remain can be resolved in the corresponding $^{13}C^{Me}$-$^{1}H^{ring}$ spectrum (Figure 2B) as there is no apparent correlation between the ^{13}CO and $^{13}C^{Me}$ chemical shifts. For smaller oligosaccharides these two sub-spectra can be acquired in a relatively short period of time with excellent signal to noise and resolution in both dimensions.

For larger oligosaccharides, correlations in the 3D version of the (H)C_{Me}COH-HEHAHA spectrum are likely to be well resolved. Figure 2C shows a ^{13}CO-$^{1}H^{ring}$ plane from the 3D spectrum of the oligosaccharide (1) taken at a $^{13}C^{Me}$ chemical shift of 21.30 ppm (marked with an arrow in Figure 2B). In the 2D $^{13}C^{Me}$-$^{1}H^{ring}$ spectrum the signals from the acetyl groups at the C2 and C4 positions of Glc (B) are exactly coincident but in the 3D spectrum they are clearly resolved with the C4 ^{13}CO at 169.35 ppm and the ^{13}CO of the C2 substituent at 170.57 ppm. The acetyl groups at the C2 and C4 positions show correlations to all other sugar ring protons, although the relative intensities differ. Any spectral overlap that remains in this experiment can be resolved in an alternative 3D experiment, the H(C_{Me})COH-HEHAHA. This experiment detects the methyl protons of the acetyl groups instead of the methyl carbons in the first evolution period (data not shown). Alternatively, the 4D version of the sequence shown in Figure 1A that correlates all three frequencies of the acetyl groups with the ring protons can be created by simply including an incremented evolution delay in the first ^{1}H-^{13}C transfer step (not shown).

The in-phase nature of the correlation peaks in the HEHAHA experiments means that accurate ^{1}H-^{1}H coupling constants can be obtained for almost the complete sugar ring spin system, even in the 3D spectrum. The values for those protons at sites that are not acetylated, which include the anomeric proton, the site of the glycosidic linkage and the proton at the site of cyclization, can be obtained from the relayed correlation peaks. Occasionally it will not be possible to observe all the correlations where overlap is severe or a small ^{1}H-^{1}H coupling limits magnetization transfer. In these instances the couplings may be measured by their contributions to the mutually coupled partners. In Figure 2C a correlation peak to the H1 at ∼5.4 ppm is clearly observed, originating from the C2 position. This correlation is also observed originating from the C4 position but it is substantially weaker. However, an accurate measurement of J_{H1-H2} can be obtained from the C4 acetyl group from its correlation to the H2, which is significantly more intense.

Accurate values of *J*-coupling constants can only be obtained from these Hartmann–Hahn-based experiments if the anti-phase dispersive contributions to the lineshapes that result from zero-quantum coherences are suppressed. We adopted the method proposed by Keeler and co-workers (Davis et al., 1993) that uses a period of spin locking in the presence of an inhomogeneous B_O field at the end of the Hartmann–Hahn mixing period. The inhomogeneity in the B_O field is generated by application of an adiabatically swept gradient with a trapezoidal shape. This has the advantage that complete suppression of the zero-quantum contributions is possible in a single scan. The gradient parameters required for this suppression were

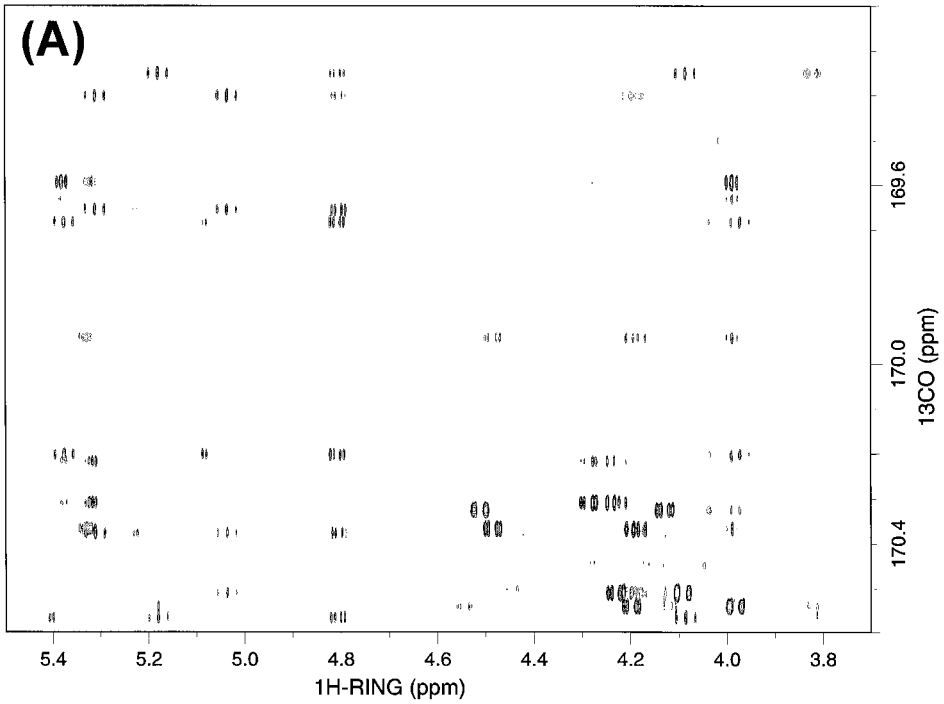

Figure 2. (A) ^{13}CO-^{1}H^{ring} spectrum recorded using a 2D version of the sequence shown in Figure 1A incrementing only t_2. Forty-eight transients were recorded for each FID to give a total acquisition time of 7 h. Data were acquired over spectral widths in F2 and F3 of 300 Hz and 2500 Hz and with 96 complex points in t_2 and 2048 complex points in t_3 and zero-filled to 512 and 4096 points, respectively before Fourier transformation. (B) ^{13}C^{Me}-^{1}H^{ring} spectrum recorded using a 2D version of the sequence shown in Figure 1A but incrementing only t_1. In this case 128 transients were collected for each of 64 increments in t_1 to give a total acquisition time of 12 h. The spectral width in F1 was 150 Hz, all other parameters were the same as in Figure 2A. (C) Part of the 3D (H)C$_{Me}$COH-HEHAHA spectrum recorded with the sequence shown in Figure 1A. This ^{13}CO-^{1}H^{ring} plane is taken at the ^{13}C^{Me}shift of 21.3 ppm which corresponds to the position marked with an arrow in Figure 2B. Data were acquired with 32, 32 and 2048 complex data points over spectral widths of 150 Hz, 300 Hz and 2400 Hz in F1, F2 and F3, respectively. Thirty-two transients were recorded for each FID to give a total acquisition time of 96 h. Spectral resolution was improved in the F1 and F2 dimensions by linear prediction to 64 and 64 points, respectively. Data were zero-filled to 128, 128 and 4096 points prior to Fourier transformation. This section shows correlations from C2 and C4 of glucose (B). A cross-section through the correlations from C4 is shown above the spectrum and the identity of the ring protons involved in the correlations is indicated in bold.

calibrated from homonuclear TOCSY experiments using the same zero-quantum suppression technique. The narrow range of chemical shifts present in these samples requires a relatively long period (30 ms) to completely de-phase the unwanted contributions in these experiments. This leads to a reduction in the overall signal intensity due to relaxation. However, in spectra recorded with a purge pulse or other simple z-filters we observed significant discrepancies between the ^{1}H-^{1}H coupling constants compared to those values measured in a 1D spectrum (data not shown). The coupling constants measured in the spectrum recorded with the adiabatic gradient sweep (Table 1) are essentially identical to those measured in the 1D spectrum except for some correlations between H5 and H6. Presumably this is because of the very similar chemical shifts, which result in a very low frequency contribution from the zero-quantum coherences which do not have time to de-phase during the 'suppression' delay.

Starting points for making chemical shift assignments in the HEHAHA experiments are provided by particular ring protons. The anomeric protons have only a single coupling to the adjacent proton, H2, and show up as a characteristic doublet (Figure 2C). In contrast, all other coherences have more complex multiplet structures. Correlations involving the H6/H6′ in hexoses and/or H5/H5′ in pentose sugars exhibit a large coupling constant of -11 to -13 Hz which can readily be distinguished from other correlations. Using these correlations it is relatively easy to trace the paths of coherence transfer from the sites of acetylation and obtain almost all the chemical shift assignments from a single spectrum.

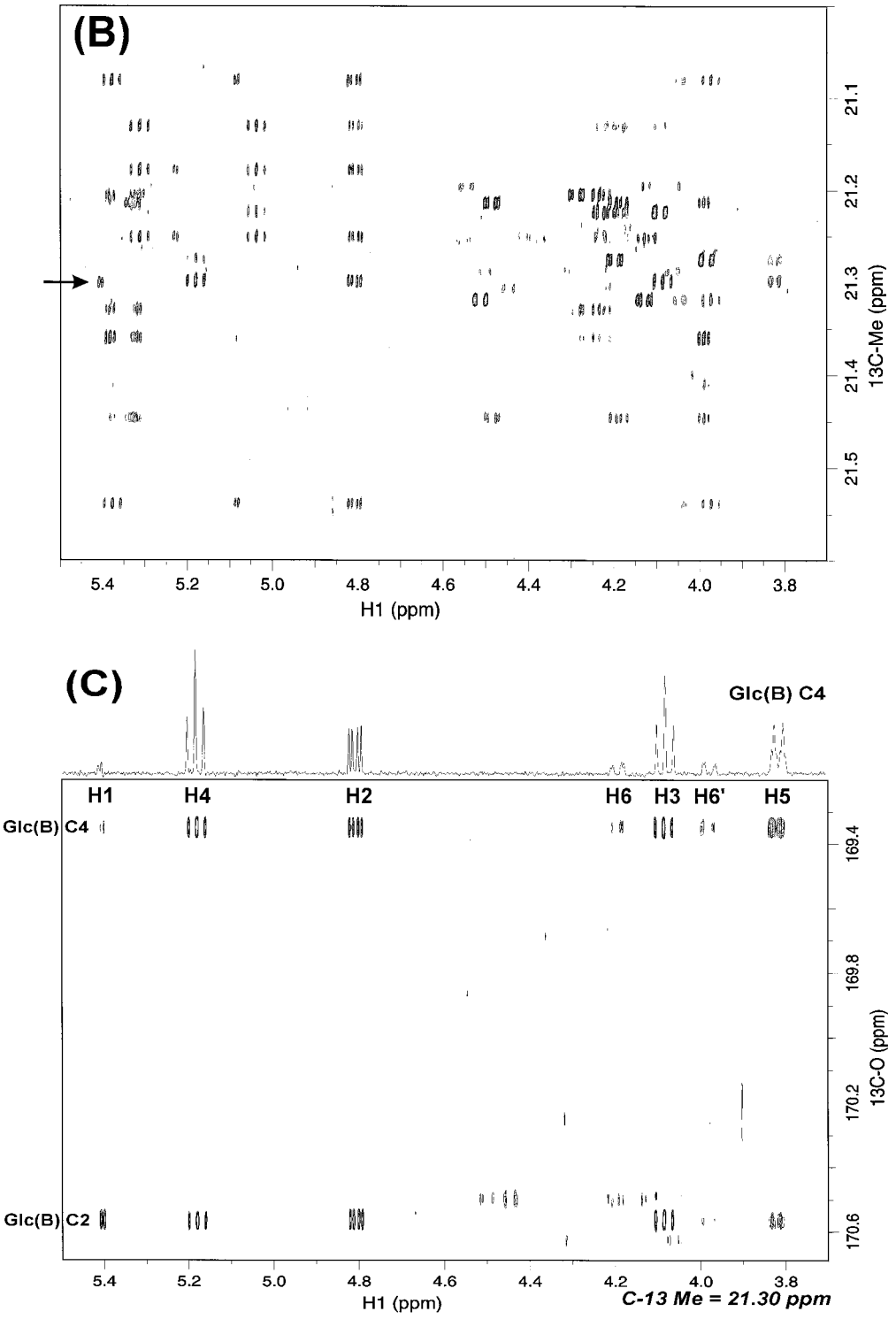

Figure 2. (continued).

Table 1. Values of coupling constants measured directly from the HEHAHA-based experiments

J-value	Sugar residue			
	Glc-A	Glc-B	Glc-C	Glc-ol(D)
$J_{11'}$	–	–	–	−12.2
$J_{1',2}$	–	–	–	7.3
$J_{1,2}$	3.7	3.9	3.8	3.4
$J_{2,3}$	10.3	10.2	10.2	5.5
$J_{3,4}$	9.5	9.5	8.8	5.5
$J_{4,5}$	10.1	10.1	9.8	4.0
$J_{5,6}$	4.1	3.4	1.5*	3.4
$J_{5,6'}$	1.6*	2.2*	3.8	7.2
$J_{6,6'}$	−12.2	−12.4	−12.3	−12.2

Values denoted with a * show significant differences from values measured in other experiments. The error in the measurements is ± 0.2 Hz. The designation of H6 and H6′ is based solely on chemical shift and not stereochemistry. H6′ is the most upfield shifted of the pair of protons.

From the values of the ^{1}H-^{1}H coupling constants it is possible to determine the stereochemistry of the sugar rings. Using the values for Glc (B) in Table 1 as an example, the coupling of 10.3 Hz between H2 and H3 implies that these protons must be oriented axially with respect to each other. Similar arguments hold for the relative stereochemistry of H3 and H4, and H4 and H5. This implies that all of these protons must be in axial positions around the sugar ring. The smaller coupling between H1 and H2 of 3.9 Hz therefore places the H1 in an equatorial position, defining this sugar as an α-pyranose sugar. The couplings between H5 and H6/H6′ do not define any of the stereochemistry of the ring.

(HC_{Me})COH and (HC_{Me})COH-RELAY

The (HC_{Me})COH and (HC_{Me})COH-RELAY experiments provide additional approaches for making chemical shift assignments in ^{13}C *O*-acetylated oligosaccharides. These experiments are useful for resolving ambiguities in those cases where the additional homonuclear transfer present in the HEHAHA-based experiments leads to significant resonance overlap. In the (HC_{Me})COH and (HC_{Me})COH-RELAY, magnetization transfer between the acetyl groups and ring protons is limited to the protons at the site of acetylation and those protons immediately adjacent to those sites, respectively.

(HC_{Me})COH

The (HC_{Me})COH experiment (Figure 1B) correlates the acetyl carbons with the ring proton at the site of acetylation. Magnetization is transferred from the $^1H^{Me}$ to ^{13}CO in the same manner described above for the HEHAHA experiments. After detecting the ^{13}CO magnetization during the evolution time t_1, the INEPT period (2∗Δ5) is used to convert the magnetization into CO_yH_Z. At the same time the anti-phase component, $C_z^{Me}CO_y$, is refocused by application of a selective 180° pulse (seduce-1 profile (McCoy and Mueller, 1993)) to the $^{13}C^{Me}$ after a period of $\sim 1/4J_{CO-C}$ (Δ4). A final INEPT period (2∗Δ6) is used to generate observable ^{1}H magnetization. A purge pulse applied immediately prior to acquisition is used to remove any undesired coherences.

Figure 3A shows the ^{13}CO-^{1}H plane of the (HC_{Me})COH experiment. In this spectrum there is only a single correlation peak for each site of acetylation and these correspond to the peaks seen in the heteronuclear COSY spectrum (Bendiak, 1999). Unlike the heteronuclear COSY spectrum the correlation peaks are in-phase and pure absorption in the indirectly detected dimension. Consequently, the resolution in this dimension is very high and in most cases it will be possible to obtain unambiguous assignments of the ^{13}CO-$^1H^{ring}$ pairs from the 2D version of this experiment. In larger oligosaccharides it may be necessary to extend these experiments to higher dimensions to resolve any overlap by including evolution periods for the $^{13}C^{Me}$ and/or $^1H^{Me}$ in the same way as outlined above.

The correlation peaks of the (HC_{Me})COH are modulated by ^{1}H-^{1}H couplings in the acquired proton dimension. During the last INEPT transfer period (2∗Δ6), magnetization is modulated both by the ^{13}CO-^{1}H couplings and by ^{1}H-^{1}H couplings. This leads to the development of antiphase terms of the type $H_y^aH_z^b$, where H^a represents protons at the site of acetylation and H^b other protons adjacent to the site of acetylation. The range of ^{13}CO-^{1}H couplings (2.5–4.7 Hz) and ^{1}H-^{1}H couplings (1–12 Hz) present means that the choice of Δ6 necessarily represents a compromise value. Calculations of the signal intensity as a function of Δ6 versus J_{CO-H} and J_{HH} suggest that there is no single value of Δ6 that provides adequate signal for the range of couplings present. Therefore the net intensity of the correlation peaks is very sensitive to the combination of coupling constants present for each group. For some combinations the intensity is positive, for others it is negative and for other combinations the net intensity will be close to zero. However, this spectrum is very sensitive and it is pos-

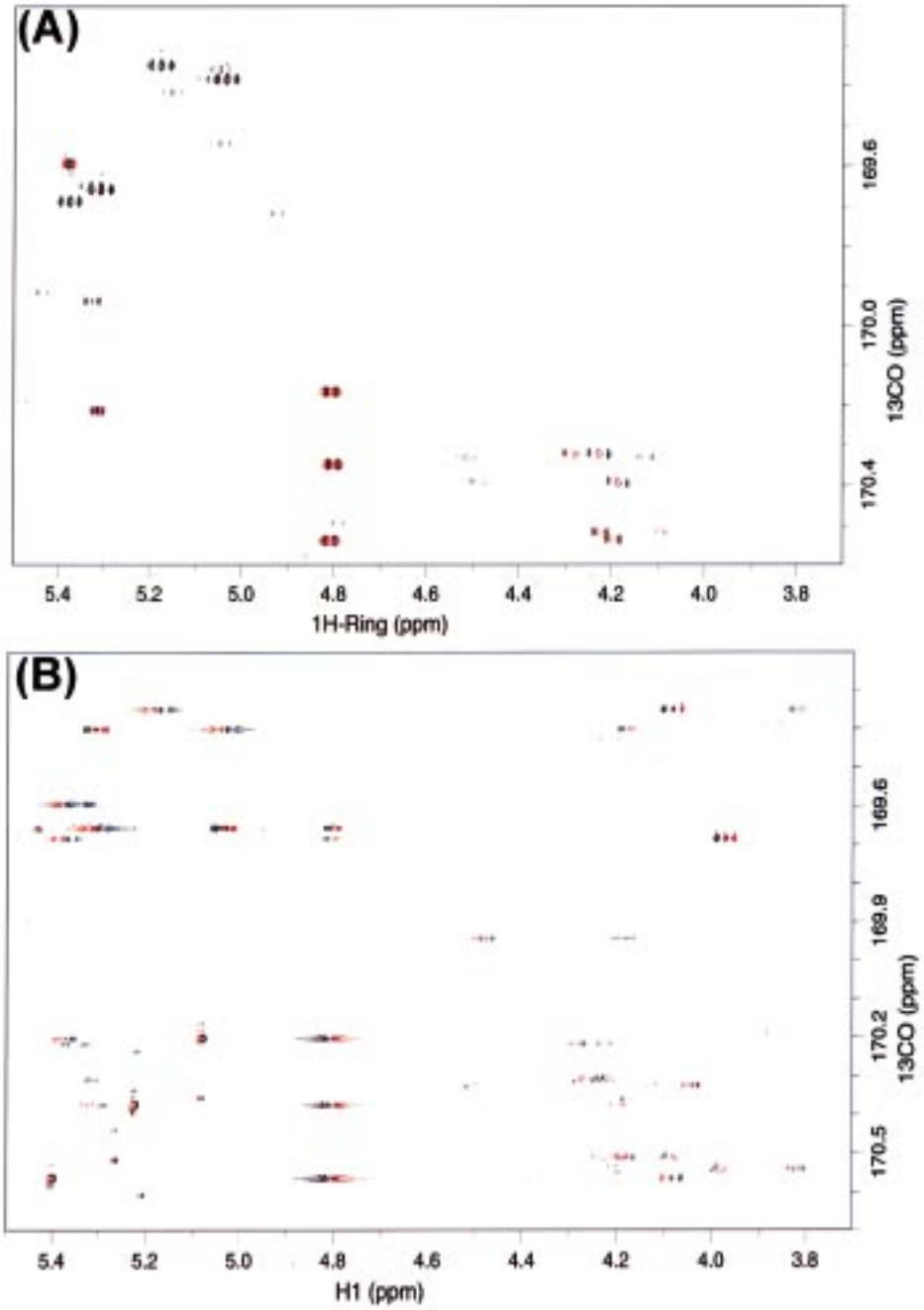

Figure 3. (A) The (HC_{Me})COH spectrum recorded using the sequence shown in Figure 1B. In this experiment delays $\Delta 5$ and $\Delta 6$ were both set to 65 ms. 128 complex points were acquired in t_1 with 8 scans per increment to give a total acquisition time of <2 h. The spectral widths in F1 and F2 were 400 Hz and 2500 Hz, respectively. Data were zero-filled to 512 points and 4096 points, respectively. (B) The (HC_{Me})COH-RELAY spectrum recorded using the sequence shown in Figure 1B with the modification described in the text. In this experiment delays $\Delta 5$ and $\Delta 6$ were both set to 65 ms. 128 complex points were acquired in t_1 with 32 scans per increment to give a total acquisition time of 6.5 h. The spectral widths in F1 and F2 were 300 Hz and 2500 Hz, respectively. Data were zero-filled to 512 points and 4096 points, respectively.

sible to collect several spectra with different values of $\Delta 6$ in a short period of time. The spectrum in Figure 3A was recorded with only 8 scans per increment in less than 2 h. If the final period $2*\Delta 6$ is omitted, the intensity of the correlation peaks depends only on the range of ^{13}CO-^{1}H couplings and the value of $\Delta 5$. If $\Delta 5$ is set to $\sim$70 ms, this retains $>$80% of the signal intensity for all of the ^{13}CO-^{1}H couplings present (neglecting the effects of relaxation). In the spectrum recorded in this manner the correlation peaks are antiphase with respect to the ^{13}CO-^{1}H coupling in the ^{1}H dimension (data not shown).

(HC$_{Me}$)COH-RELAY

The (HC$_{Me}$)COH-RELAY experiment correlates the acetyl groups with the sugar ring protons immediately adjacent to the site of acetylation. The pulse sequence for the (HC$_{Me}$)COH-RELAY is created by replacing the spin-lock pulse in Figure 1B with a 90°_{x} ^{1}H pulse. Now the antiphase terms $H^{a}_{y}H^{b}_{z}$ that develop during the final INEPT period ($2*\Delta 6$) are converted into observable magnetization of the type $H^{a}_{z}H^{b}_{y}$. The resulting spectrum (Figure 3B) contains both the direct correlation between the acetyl groups and ring protons at the site of acetylation and relayed correlations to protons adjacent to the sites of acetylation. Again the intensities of the correlations will depend on the magnitude of both the ^{13}CO-^{1}H couplings and the ^{1}H-^{1}H couplings present. However, in this case a compromise value of $\Delta 6 = 60$–80 ms will retain $>$50% of the desired coherences across the complete range of both the ^{13}CO-^{1}H and ^{1}H-^{1}H couplings present in these oligosaccharides. The direct correlations to protons at the site of acetylation are also observed, as they are partially retained by the use of a compromise value for $\Delta 6$. The 'relayed' correlations are antiphase with respect to J_{HaHb} and are 90° out of phase relative to the 'direct' correlations. The antiphase splittings in the correlation peaks are only present in the directly detected dimension, which can be collected with sufficient digital resolution to minimize problems with cancellation. Again problems with overlap can be minimized by recording 3D versions of the experiment in an analogous manner to the HEHAHA-based experiments outlined above.

Discussion

We have shown that ^{13}C *O*-acetylation in combination with multi-dimensional NMR spectroscopy is a powerful method for obtaining primary structure information of oligosaccharides. These four new NMR experiments, the (H)C$_{Me}$COH-HEHAHA, H(C$_{Me}$)COH-HEHAHA, (HC$_{Me}$)COH and (HC$_{Me}$)COH-RELAY, provide multiple approaches to establish correlations between ^{13}C-labeled acetyl groups and protons on the sugar ring. We have demonstrated the feasibility of these experiments by the study of a tetrasaccharide to determine both chemical shift assignments and ring stereochemistry.

The characterization of oligosaccharide structures requires a knowledge of the identity of the individual sugar rings, the stereochemistry at the anomeric positions and the positions of the linkages between the individual sugars. The (H)C$_{Me}$COH-HEHAHA and H(C$_{Me}$)COH-HEHAHA experiments contain much of the essential information required for a complete structural characterization of the molecule. These two experiments use a heteronuclear Hartmann–Hahn (HEHAHA) mixing sequence to transfer magnetization from the acetyl groups to protons on the sugar ring. The use of HEHAHA mixing sequences is particularly advantageous for the study of *O*-acetylated oligosaccharides: (i) the correlation peaks are in-phase and pure absorption in all dimensions and so do not suffer from problems of cancellation; (ii) the spectrum contains correlations to almost all the individual sugar ring protons from each site of acetylation. If a sugar ring has more than one free hydroxyl group, then in the final spectrum of the *O*-acetylated molecule there will be multiple sets of correlations. This redundancy in the information content is of considerable benefit if there is either significant resonance overlap or if the coupling constant between adjacent ring protons is small ($<$1–2 Hz). In the latter case magnetization transfer through the small coupling is inefficient and not all the correlations from each acetyl group are observed. As a result it is possible to determine both the chemical shift assignments and the ^{1}H-^{1}H coupling constants from just a single experiment.

The (HC$_{Me}$)COH and (HC$_{Me}$)COH-RELAY experiments are designed to identify the sites of acetylation in peracetylated oligosaccharides and by inference the ring positions involved in the formation of glycosidic linkages. The (HC$_{Me}$)COH spectrum establishes the direct correlation between the acetyl substituent and the ring proton at the site of acetylation. Although this information was previously obtained from heteronuclear COSY and HMBC experiments (Bendiak, 1999), the (HC$_{Me}$)COH experiment presented here has higher sensitivity and greater reso-

lution as the correlation peaks are not broadened by the presence of the ^{13}CO-$^{1}H^{ring}$ coupling in the indirect dimensions. The (HC_{Me})COH-RELAY spectrum helps to assign the sites of acetylation by identifying those protons immediately adjacent to the site of acetylation. These experiments provide only limited information about ^{1}H-^{1}H *J*-coupling constants that are required to define the stereochemistry of the sugar rings because of the mixed phase of the correlation peaks.

The experiments presented here are designed to help characterize the primary structure of oligosaccharides. They provide information about the stereochemistry of the individual rings and also the location of sites of substitution that are likely to be involved in the formation of the inter-sugar glycosidic linkage. However, complex carbohydrates may contain non-carbohydrate substituents in which case additional analysis such as mass spectrometry may be required to completely characterize the molecule. The sequence of sugar residues along the oligosaccharide chain can be established from the rotating frame NOEs between sugars involved in glycosidic bonds observed in ROESY experiments (Dabrowski et al., 1989), which, when used in combination with the methods presented here, should permit most structures to be elucidated.

This work demonstrates the use of ^{13}C *O*-acetylation to introduce up to three new independent frequency dimensions that can be exploited to significantly reduce the problems of spectral overlap encountered with larger oligosaccharides. This method of ^{13}C labeling has the advantage that it can be applied to any oligosaccharide and is not limited to samples produced from cell cultures. Furthermore, it can also be applied efficiently in cases where sample quantity would usually limit the NMR experiments that could be performed. Acetylation is not limited to oligosaccharides but can in principle be applied to any molecules that have free functional groups amenable to acetylation. The extra resolution that is obtained by the introduction of two ^{13}C nuclei with very distinct chemical shifts makes it possible to extend the size range of oligosaccharides that can be studied by NMR spectroscopy. The use of pulse sequences that retain pure-absorption in-phase coherences in the final spectrum significantly enhances both the quality and reliability of the information that can now be obtained for these molecules. We are presently investigating the application of these experiments to molecules containing 10–20 sugar residues.

Acknowledgements

We would like to thank James Keeler for his advice on zero-quantum suppression techniques and Mair Churchill for her helpful comments and suggestions in the preparation of this manuscript. The authors thank the University of Colorado Cancer Center Core grant NIH5P30-CA46934-10 and the Howard Hughes Medical Institute for providing funds for spectrometers used in these studies.

References

Baum, J., Tycko, R. and Pines, A. (1985) *Phys. Rev.*, **A32**, 3435–3447.

Bearden, D.W. and Brown, L.R. (1989) *Chem. Phys. Lett.*, **163**, 432–436.

Bendiak, B. (1999) *Carbohydr. Res.*, **315**, 206–221.

Boyd, J. and Soffe, N. (1989) *J. Magn. Reson.*, **85**, 406–413.

Braunschweiler, L. and Ernst, R.R. (1983) *J. Magn. Reson.*, **53**, 521–528.

Brown, L.R. and Sanctuary, B.C. (1991) *J. Magn. Reson.*, **91**, 413–421.

Chui, D., Oh-Eda, M., Liao, Y.F., Panneerselvam, K., Lal, A., Marek, K.W., Freeze, H.H., Moremen, K.W., Fukuda, M.N. and Marth, J.D. (1997) *Cell*, **90**, 157–167.

Dabrowski, J., Ejchart, A., Bruntz, R. and Egge, H. (1989) *FEBS Lett.*, **246**, 229–232.

Darvill, A., Bergmann, C., Cervone, F., DeLorenzo, G., Ham, K.S., Spiro, M.D., York, W.S. and Albersheim, P. (1994) *Biochem. Soc. Symp.*, **60**, 89–94.

Davis, A.L., Estcourt, G., Keeler, J., Laue, E.D. and Titman, J.J. (1993) *J. Magn. Reson.*, **A105**, 167–183.

Emsley, L. and Bodenhausen, G. (1992) *J. Magn. Reson.*, **97**, 135–148.

Ernst, M., Griesinger, C., Ernst, R.R. and Bermel, W. (1991) *Mol. Phys.*, **74**, 219–252.

Ernst, R.R., Bodenhausen, G. and Wokaun, A. (1987) *Principles of Nuclear Magnetic Resonance in One and Two Dimensions*, Clarendon Press, Oxford.

Geen, H. and Freeman, R. (1991) *J. Magn. Reson.*, **93**, 93–141.

Hennet, T., Chui, D., Paulson, J.C. and Marth, J.D. (1998) *Proc. Natl. Acad. Sci. USA*, **95**, 4504–4509.

Hileman, R.E., Fromm, J.R., Weiler, J.M. and Linhardt, R.J. (1998) *BioEssays*, **20**, 156–167.

Homeister, J.W., Zhang, M., Frenette, P.S., Hynes, R.O., Wagner, D.D., Lowe, J.B. and Marks, R.M. (1998) *Blood*, **92**, 2345–2352.

Hounsell, E.F., Young, M. and Davies, J. (1997) *Clin. Sci.*, **93**, 287–293.

Hwang, T.L. and Shaka, A.J. (1995) *J. Magn. Reson.*, **A112**, 275–279.

Kellogg, G.W. (1992) *J. Magn. Reson.*, **98**, 176–182.

Kellogg, G.W. and Schweitzer, B.I. (1993) *J. Biomol. NMR*, **3**, 577–595.

Kupce, E. and Freeman, R. (1997) *J. Magn. Reson.*, **127**, 36–48.

Majumdar, A., Wang, H., Morshauser, R.C. and Zuiderweg, E.R.P. (1993) *J. Biomol. NMR*, **3**, 387–397.

Marion, D., Ikura, M., Tschudin, R. and Bax, A. (1989) *J. Magn. Reson.*, **85**, 393–399.

McCoy, M.A. and Mueller, L. (1993) *J. Magn. Reson.*, **A101**, 122–130.
Metzler, M., Gertz, A., Sarkar, M., Schachter, H., Schrader, J.W. and Marth, J.D. (1994) *EMBO J.*, **13**, 2056–2065.
Nikonowicz, E.P. and Pardi, A. (1993) *J. Mol. Biol.*, **232**, 1141–1156.
Patt, S.L. (1992) *J. Magn. Reson.*, **96**, 94–102.
Richardson, J.M., Clowes, R.T., Boucher, W., Domaille, P.J., Hardman, C.H., Keeler, J. and Laue, E.D. (1993) *J. Magn. Reson.*, **B101**, 223–227.
Schweitzer, B.I., Gardner, K.H. and Tucker-Kellogg, G. (1995) *J. Biomol. NMR*, **6**, 180–188.
Shaka, A.J., Keeler, J., Frenkiel, T. and Freeman, R. (1983) *J. Magn. Reson.*, **52**, 335–338.
Shaka, A.J., Lee, C.J. and Pines, A. (1988) *J. Magn. Reson.*, **77**, 274–293.
Silver, M.S., Joseph, R.I. and Hoult, D.I. (1984) *J. Magn. Reson.*, **59**, 347–351.
Sklenar, V., Dieckmann, T., Butcher, S.E. and Feigon, J. (1996) *J. Biomol. NMR*, **7**, 83–87.
Tan, J., Dunn, J., Jaeken, J. and Schachter, H. (1996) *Am. J. Human Genet.*, **59**, 810–817.
Wang, H. and Zuiderweg, E.R.P. (1995) *J. Biomol. NMR*, **5**, 207–211.
Wijmenga, S.S., Heus, H.A., Leeuw, H.A.E., Hoppe, H., Van der Graaf, M. and Hilbers, C.W. (1995) *J. Biomol. NMR*, **5**, 82–86.
Zuiderweg, E.R.P. (1990) *J. Magn. Reson.*, **89**, 533–542.
Zuiderweg, E.R.P., Zeng, L., Brutscher, B. and Morshauser, R.C. (1996) *J. Biomol. NMR*, **8**, 147–160.